

# FYS4150 Project 5:

## *N*-body simulation of an open cluster

Marie Foss (# 56), Maria Hammerstrøm (# 59)

### Abstract

Lorem ipsum dolor sit amet, consectetur adipiscing elit. Ut purus elit, vestibulum ut, placerat ac, adipiscing vitae, felis. Curabitur dictum gravida mauris. Nam arcu libero, nonummy eget, consectetur id, vulputate a, magna. Donec vehicula augue eu neque. Pellentesque habitant morbi tristique senectus et netus et malesuada fames ac turpis egestas. Mauris ut leo. Cras viverra metus rhoncus sem. Nulla et lectus vestibulum urna fringilla ultrices. Phasellus eu tellus sit amet tortor gravida placerat. Integer sapien est, iaculis in, pretium quis, viverra ac, nunc. Praesent eget sem vel leo ultrices bibendum. Aenean faucibus. Morbi dolor nulla, malesuada eu, pulvinar at, mollis ac, nulla. Curabitur auctor semper nulla. Donec varius orci eget risus. Duis nibh mi, congue eu, accumsan eleifend, sagittis quis, diam. Duis eget orci sit amet orci dignissim rutrum.

**Github:** <https://github.com/mariahammerstrom/Project5>

## 1 Introduction

An open cluster is a group of up to a few thousand stars that are gravitationally bound to each other. These stars are created from the same giant molecular cloud, making the age and composition of the stars similar, which in turn makes the properties of the stars, such as distance, age, metallicity and extinction, more easy to determine.

Open clusters are usually found in the arms of spiral galaxies or in irregular galaxies. Once an open cluster has formed, it will gradually dissipate as its members gets ejected from the cluster due to random collisions, lasting only a few hundred million years.

In this project we make a simple model for how an open cluster is formed from a gravitational collapse and model the interactions among a large number of stars. We have simulated a "cold collapse", meaning the stars will start at rest. The stars have masses randomly distributed by a Gaussian distribution around  $10M_{\odot}$  with a standard deviation of  $1M_{\odot}$ , and uniform randomly distributed positions within a sphere of a given radius  $R_0$ .

We first study the Newtonian two-body problem in three dimensions, then extend this to an  $N$ -body problem in three dimensions. The time evolution of the system is described through **Newton's law**, given by:

$$\frac{d^2x}{dt^2} = \frac{F_{G,x}}{M} \quad (1)$$

where  $F_{G,x}$  is the **gravitational force** in the  $x$  direction, given by

$$F_{G,x} = -\frac{GM_1M_2}{r^3}x, \quad (2)$$

where  $M_1$  and  $M_2$  are the masses of the two objects and  $r$  is the distance between them. In three dimensions,  $r = \sqrt{x^2 + y^2 + z^2}$ . We have similar expressions for the  $y$  and  $z$  direction.

Eq. (1) is a second-order differential equation, which we can rewrite as a set of coupled first-order differential equations:

$$\frac{dx}{dt} = v_x \quad \text{and} \quad \frac{dv_x}{dt} = F_{G,x}. \quad (3)$$

These equations can be used to determine the position and velocity of an object.

In the case where the number of objects  $N \rightarrow \infty$  and keeping the mean density  $\rho_0$  constant, the system will collapse into a singularity at a finite **collapse time**

$$\tau_{\text{crunch}} = \sqrt{\frac{3\pi}{32G\rho_0}}, \quad (4)$$

derived in Appendix A.2. We can write  $G$  in units of  $\tau_{\text{crunch}}$  so that  $G$  becomes a function of the number of particles  $N$  and the average mass of the particles  $\mu$ , which gives

$$SOMETHING \quad (5)$$

which is derived in the Appendix A.3.

After running calculations for the gravitational force as expressed in Eq. (2), we introduce a smoothing function to take care of any numerical instability that may arise when two stars come very close. We modify the gravitational force as

$$F_{G,\text{mod}} = -\frac{GM_1M_2}{r^2 + \epsilon^2}, \quad (6)$$

where  $\epsilon$  is a small real constant. We will try out different values for  $\epsilon$ .

The **virial theorem** says that for a bound gravitational system in equilibrium we have

$$2\langle K \rangle = -\langle V \rangle, \quad (7)$$

where  $\langle K \rangle$  is the time-averaged kinetic energy of the system and  $\langle V \rangle$  is the time-averaged potential energy of the system. The virial theorem deploys the ergodic hypothesis, which states that we can take an ensemble average instead of a time average. By

calculating the kinetic and potential energy of our system, we can check if our results are consistent with Eq. (7).

Finally we wish to study the **radial density** of the particles in the equilibrium state. This can be calculated from our computations and be fitted with the simple expression

$$n(r) = \frac{n_0}{1 + (\frac{r}{r_0})^4} \quad (8)$$

where  $n_0$  and  $r_0$  are scaling constants. The result can also be compared with the well-known Navarro-Frenk-White profile

$$\rho(r) = \frac{\rho_0}{\frac{r}{r_0}(1 + \frac{r}{r_0})^2}, \quad (9)$$

where  $\rho_0$  and  $r_0$  are scaling constants.

## 2 Methods

The numerical algorithms we wish to implement and compare are the fourth-order Runge-Kutta method and the Velocity-Verlet method. Both methods assume a known initial value for the position  $(x_i, y_i, z_i)$  and the velocity  $(v_{i,x}, v_{i,y}, v_{i,z})$ . Both methods are self-starting.

### 2.1 4th order Runge-Kutta method

Using the 4th order Runge-Kutta method (RK4), we can estimate the next value  $x_{i+1}$  (and similarly  $y_{i+1}$  and  $z_{i+1}$ ) through the formula

$$x_{i+1} \approx x_i + \frac{h}{6}(v_{i,x} + 2v_{i+1/2,x} + 2v_{i+1/2,x} + v_{i+1,x}), \quad (10)$$

where  $v_{i+1/2,x}$  is the velocity in the  $x$  direction at time  $t_{i+1/2}$  and position  $x_{i+1/2}$  after taking a step  $h/2$ , which marks the midpoint between  $v_{i,x}$  and  $v_{i+1,x}$ . The midpoint is evaluated two times to get a better estimate of the function value at this point, which in turn will give a better estimate for the final point  $v_{i+1,x}$ .  $h$  denotes the time step, defined as  $h = (t_f - t_0)/N$  where  $t_f$  is the end-time of our simulation,  $t_0$  is the start-time (usually chosen as zero), and  $N$  is the number of integration points (not to be confused with the number of particles in the simulation!).

The algorithm goes as follows:

- Compute  $K_1 = h v_x(t_i, x_i)$ , which gives the slope at  $t_i$ .
- Compute the slope at the midpoint using Euler's method, which gives  $K_2 = h v_x(t_i + h/2, x_i + K_1/2)$ .
- The estimate of the slope at the midpoint is then further improved by  $K_3 = h v_x(t_i + h/2, x_i + K_2/2)$ .
- Finally compute the end-point through:  
 $x_{i+1} = x_i + \frac{1}{6}(K_1 + 2K_2 + 2K_3 + K_4)$ .

These equations must be deployed for all three dimensions  $x, y$  and  $z$ .

Using this method gives a global truncating error which goes like  $O(h^4)$ .

### 2.2 Velocity-Verlet

This method is derived by performing a Taylor expansion of  $x(t + h)$ , which in discretized notation can be written as

$$x_{i+1} = x_i + v_i \Delta t + \frac{\Delta t^2}{2} a_i, \quad (11)$$

where  $a_i$  is the acceleration and  $\Delta t$  is the time step.

For this method the next step in the velocity is calculated by

$$v_{i+1} = v_i + \frac{1}{2} \Delta t (a_i + a_{i+1}), \quad (12)$$

where  $a_{i+1}$  is the acceleration calculated using  $x_{i+1}$ . Thus the algorithm can be summed up as:

- Given the initial position  $x_0$  and velocity  $v_0$  at time  $t = t_0 = 0$ , calculate the next position  $x_1$  using Eq. (11).
- Calculate  $a_1$  from the interacting forces using the new position  $x_1$ .
- Calculate  $v_1$  as described in Eq. (12) given  $a_1$ .
- Increase the time step, so that  $t = t_0 + \Delta t$ .
- Keep calculating  $x_{i+1}$  and  $v_{i+1}$ , and increasing the time step, until the pre-determined final time is reached.

Using this method gives a global truncating error which goes like  $O(h^3)$  for the positions  $(x_i, y_i, z_i)$ , and  $O(h^2)$  for the velocities  $(v_{i,x}, v_{i,y}, v_{i,z})$ , thus the velocities are not approximated to the same accuracy as the positions are.

### 2.3 Random distributions

The particles in the  $N$ -body case will start with positions  $(x, y, z)$  drawn from a **random uniform distribution** within a sphere of radius  $R_0$ . Achieving this numerically is not entirely trivial if we want to avoid the particle density being much higher in the centre. First we consider the spherical representation of the co-ordinates

$$\begin{aligned} x &= r \sin\theta \cos\phi \\ y &= r \sin\theta \sin\phi \\ z &= r \cos\theta \end{aligned} \quad (13)$$

where  $\theta \in [0, \pi]$ ,  $\phi \in [0, 2\pi]$  and  $r \in [0, R_0]$ . The trick is to rewrite the volume element as

$$r^2 \sin\theta dr d\theta d\phi = A du dv dw,$$

where  $u, v, w \in [0, 1]$  and  $A$  is a constant. Following the approach of H.T. Ihle (2015), we find

$$\begin{aligned} \theta &= \arccos(1 - 2v) \\ \phi &= 2\pi w \\ r &= R_0 u^{1/3} \end{aligned} \quad (14)$$

where  $u, v, w$  are computed using the built-in C++ function `uniform_real_distribution`, which will give randomly distributed numbers in the interval  $[0, 1]$ . Then, plugging the computed values of Eq. (14) into Eq. (13) gives the desired result.

The particles will be assigned a randomly distributed mass from a **Gaussian distribution** for a given mean value  $10M_\odot$  and with a standard deviation  $M_\odot$ . This is simply done using the built-in C++ function `normal_distribution`.

## 2.4 Nondimensionalization

We use solar masses  $M_\odot$  and light years as units of mass and length to make our equations dimensionless. This results in

$$SOMETHING \quad (15)$$

which is derived in Appendix A.1.

# 3 Results

## 3.1 Testing the numerical methods

We test our implementation of the numerical methods described in Sec. 2 by running the code for a case where the analytical solution is known. In the case of a second-order differential equation like the one we have in Eq. (1), we can test our algorithm by considering a box on a spring. In this case the equation to be solved is:

$$F = -kx \Rightarrow \frac{d^2x}{dt^2} = -\frac{k}{m}x = -\omega_0^2x, \quad (16)$$

which has the known analytical solution  $x(t) = A \cos(\omega_0 t + \nu)$ , where  $\nu$  is the phase constant. The coupled first-order differential equations can in this case be written as

$$\frac{dx}{dt} = v_x \quad \text{and} \quad \frac{dv_x}{dt} = -\frac{k}{m}x. \quad (17)$$

where we can set  $k = m = 1$  for simplicity when checking the validity of our numerical methods. Then the analytical solution is simply  $x(t) = \cos(t)$ , with  $v(t) = -\sin(t)$ .

A visualization of our test is shown in Fig. 1a-d, here for time steps of  $\Delta t = 0.10$  and  $\Delta t = 1.0$ . We see that the numerical algorithms reproduce the result of the analytical expression extremely well for small time steps – it's impossible to tell the methods apart. The result is less impressive for larger time step.

Another test we can make is to check for **energy conservation**. With initial conditions  $x_0$  and  $v_0$ , we can calculate

$$\begin{aligned} E(t=0) = E_0 &= \frac{1}{2}mv_0^2 + \frac{1}{2}kx_0^2, \\ E(t=t_i) = E_i &= \frac{1}{2}mv_i^2 + \frac{1}{2}kx_i^2, \end{aligned} \quad (18)$$

and check that  $E_0 = E_i$  for every period  $T$ . It is however easier to just plot  $E_i$  as a function of time for the different methods and inspect the result. If the energy is conserved, the plot should be a straight line, as the energy should not change over time. As shown in Fig. 1e-f this is indeed the case in the analytical case. If

we look closely at the  $y$ -axis we see that this really is the case for all the methods, with the numerical methods deviating from the expected result in the fourth decimal place. For RK4 with large time steps, the energy is not conserved at all, but declines rapidly.

Now that we have verified our numerical methods, we can go on to solve the problem at hand.

## 3.2 Stability of methods

Let us first comment on the stability of the analytical case before moving on to the gravitational system. Studying the analytical case with spring force, the two methods are good estimates for time step  $h < 1$ . RK4 is slightly closer to the analytical solution. For  $h \geq 1$ , the oscillation in position and velocity is damped when using RK4. This is more visible for longer times. With the VV method, the position amplitude is 1, whereas the velocity amplitude is lowered to 0.75. Thus, for larger time steps, VV is the most stable method.

Now let us consider the Newtonian two-body problem in three dimensions. Here we have chosen a configuration close to that of the Sun-Earth system: One mass is heavy and has no velocity of its own (Sun-like object), while the other mass is much lighter with some velocity in the  $x$ -direction (Earth-like object). By trying out different relative distances  $r$  between the Sun-like and the Earth-like object, as well as different velocities in the  $x$ -direction, we can get a system where our Earth-like object follows a nice orbit around the massive object in the center. As seen in Fig. 2a-d, the orbit – or lack thereof – very much depends on the time step, especially in the case where the radius is a bit too small to make the orbit stable, visible in Fig. 2b. In general it is clear from the figures that RK4 does a better job in all cases, except in Fig. 2c where the two methods give approximately identical results.

to study the stability of the two methods described in Sec. 2. This is done by running the two algorithms over a very long time period.

...  
We also check how the two methods work for large time steps.

...  
What is also interesting is to compare the time used to advance one time step for the two different methods, to see which one is the most efficient.

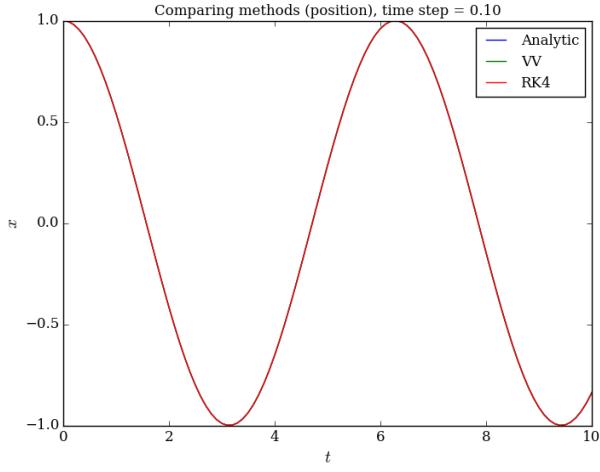
...  
Based on our study of the stability and time usage of the two methods, we can say that ... COMMENT.

We go on to look at the  $N$ -body system. For a system with  $N = 100$  and a radius  $R_0 = 20$  ly, a time step of XXXX is required.

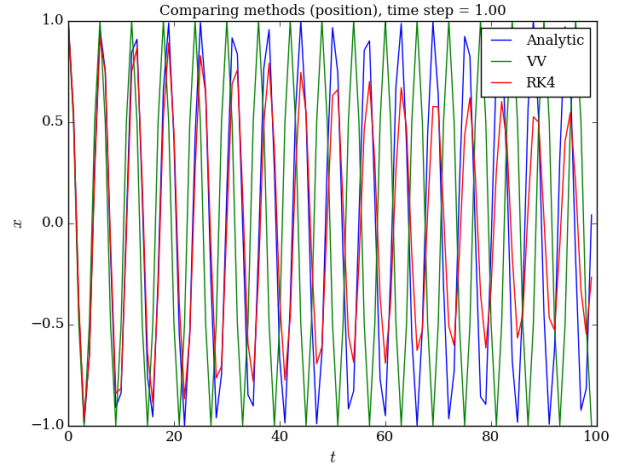
We run the calculations for both methods in Sec. 2. XXX

# 4 Conclusions

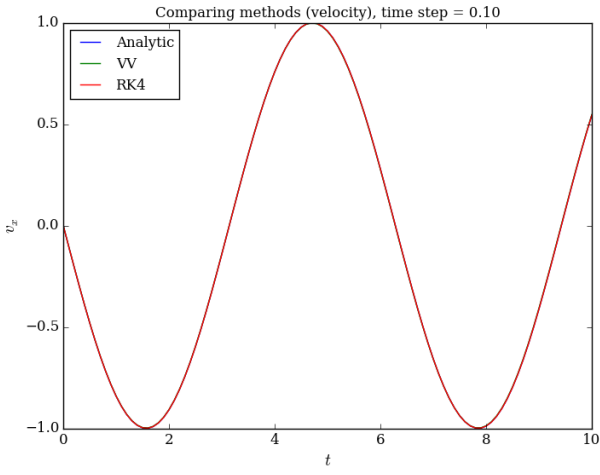
...



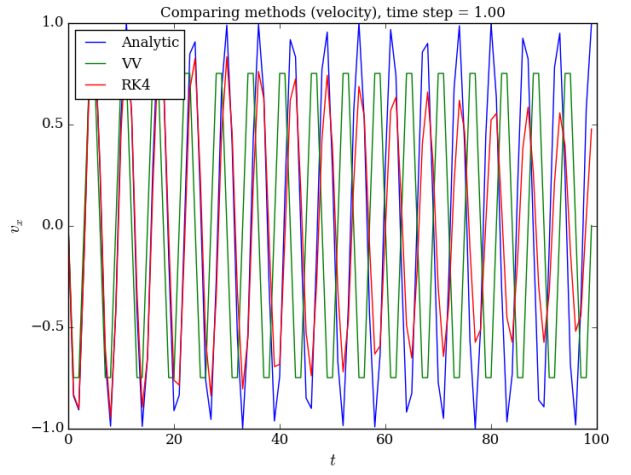
(a) Position,  $\Delta t = 0.10$



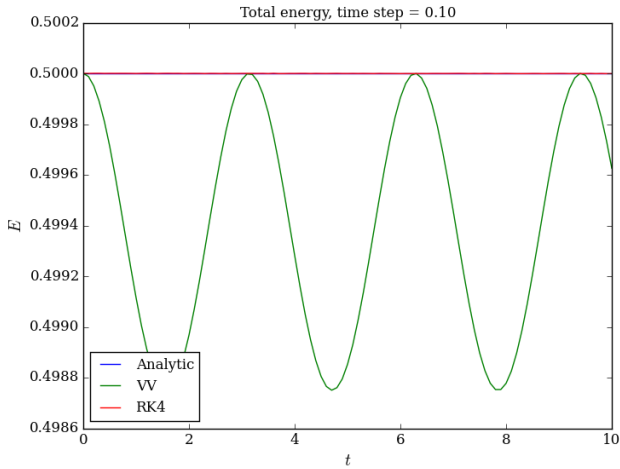
(b) Position,  $\Delta t = 1.00$



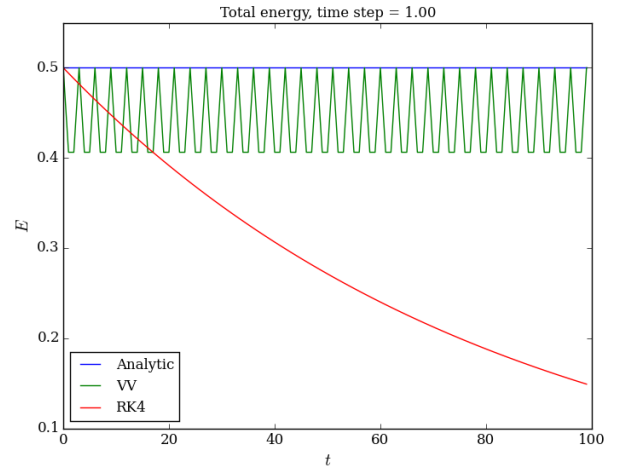
(c) Velocity,  $\Delta t = 0.10$



(d) Velocity,  $\Delta t = 1.00$

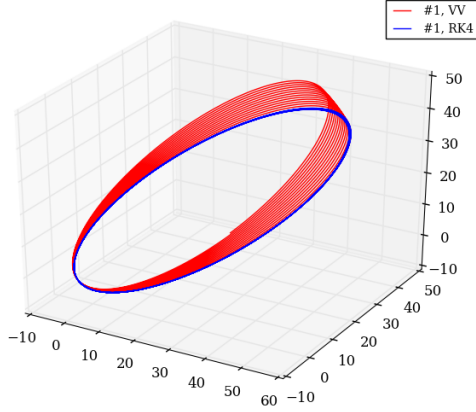


(e) Energy,  $\Delta t = 0.10$

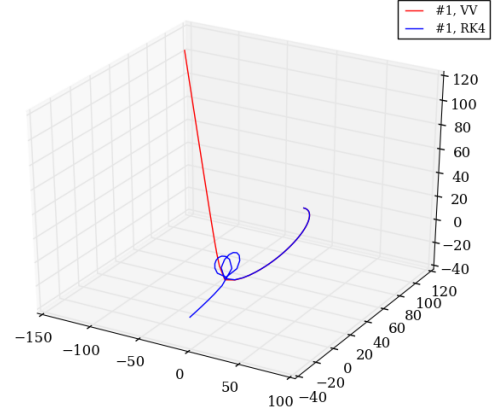


(f) Energy,  $\Delta t = 1.00$

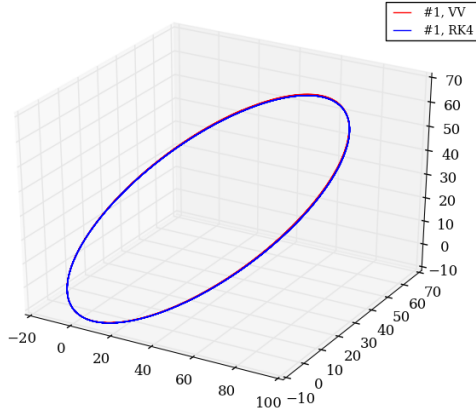
**Figure 1:** Comparison of our numerical algorithms in the analytical case of the box on a spring: Velocity-Verlet (green) and 4th-order Runge-Kutta (red), with the analytical solution (blue) are shown for two different time steps  $\Delta t = 0.10$  and  $\Delta t = 1.00$ , and for two different durations  $t_{\text{final}} = 10$  and  $t_{\text{final}} = 100$ .



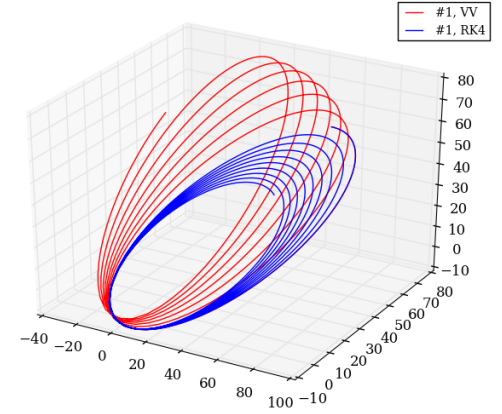
(a) Position,  $\Delta t = 0.10$ ,  $r = 40$



(b) Position,  $\Delta t = 1.00$ ,  $r = 40$



(c) Position,  $\Delta t = 0.10$ ,  $r = 60$



(c) Position,  $\Delta t = 1.00$ ,  $r = 60$

**Figure 2:** Comparison of our numerical algorithms in the 2-body case where one body is massive and sitting in the center of the orbit (not plotted): Velocity-Verlet (green) and 4th-order Runge-Kutta (red), with the analytical solution (blue), for two different time steps  $\Delta t = 0.10$  and  $\Delta t = 1.00$ , as well as two different radii,  $r = 40$  and  $r = 60$ .

## 5 List of codes

The codes developed and used in this project are:

### 5.1 *Running calculations (C++)*

- `main.cpp` – main program where the calculations are run, calling on the classes listed below.
- `solver.cpp` – class containing the numerical methods.
- `star.cpp` – class collecting various properties of the stars.
- `galaxy.cpp` – class containing all the stars in the galaxy.

### 5.2 *Plotting (Python)*

- `plotting_analytical.py` – program to graphically compare the one-dimensional 2-body problem with an analytical solution, described in Sec. 3.1.
- `plot_method.py` – program to graphically compare the two numerical methods described in Sec. 2.1 and Sec. 2.2.
- `plotting_scatter.py` – plotting program to visualize the  $N$ -body system in 3D.
- `plotting_radialprofile.py` – plotting program that calculates the radial profile of the system, fitted with the profiles in Eq. (8) and Eq. (9).

## A Appendix

### A.1 Nondimensionalization

...

### A.2 Derivation of $t_{\text{crunch}}$

...

### A.3 Rewriting of $t_{\text{crunch}}$

We want to write  $G$  in units of  $\tau_{\text{crunch}}$  so that  $G$  becomes a function of the number of particles  $N$  and the average mass of the

particles  $\mu$ . Inverting Eq. (4) with respect to  $G$ , gives

$$G = \frac{3\pi}{32\rho_0} \frac{1}{\tau_{\text{crunch}}^2}, \quad (19)$$

where we can replace  $\rho_0$  by using that

$$\mu = \frac{\bar{M}}{M_\odot} = \frac{\rho_0}{NM_\odot} \Rightarrow \rho_0 = \mu NM_\odot, \quad (20)$$

where  $N$  is the total number of particles and  $\bar{M}$  is the average mass of the system. Then we can rewrite Eq. (19) as

$$G = \frac{3\pi}{32\mu NM_\odot} \frac{1}{\tau_{\text{crunch}}^2}. \quad (21)$$